

# Life Span Studies on Functionally Graded Composite Coatings

Abhinav<sup>\*</sup>, Rahul Ribeiro<sup>\*\*</sup>, Abhijeet Hugar<sup>\*\*</sup>

<sup>\*</sup> Department of Mechanical Engineering, Alliance College of Engineering and Design, Alliance University

<sup>\*\*</sup> Department of Mechanical Engineering, Alliance College of Engineering and Design, Alliance University

**Abstract-** The present paper examines the failure mechanism of the coating system of  $\text{Al}_2\text{O}_3\text{-ZrO}_2 \cdot 5\text{CaO}$  applied on a Cast iron (CI) substrate. Atmospheric plasma spray coating technique was used for coating applications. Muffle furnace was used to heat the sample at  $600 \pm 2^\circ\text{C}$  followed by ambient cooling. Both the heating and cooling cycle was maintained for 30 minutes. Results were compared with the as-sprayed coated specimen with the post thermal cyclic test specimen. It has been noticed that normal stresses developed due to the formation of thermally grown oxide (TGO) at the interface of the top/bond coat and institute the weakest link in the coating system. Also due to differential porosity at the interface led the moisture to penetrate from the top coat to bottom coat thus thermochemical effect commenced underneath the bond coat, leading to the formation of oxides and made the top coat gradually more brittle during the thermal cyclic process.

**Index Terms-** Muffle furnace,  $\text{Al}_2\text{O}_3\text{-ZrO}_2 \cdot 5\text{CaO}$ , thermochemical, thermally grown oxide.

## I. INTRODUCTION

Thermal barrier coatings (TBCs) often used to protect the components subjected to high-temperature applications viz. gas turbine engines, internal combustion parts, etc. [1]. In the previous studies it has been found that yttria stabilized zirconia failed due to the phase transformation from tetra,  $t\text{-ZrO}_2$  to monoclinic,  $m\text{-ZrO}_2$  [2]. Attention is required to improve the thermal cyclic behavior by appropriate material composition. Fracture response and thermal resistance of yttria-stabilized zirconia (YSZ)–NiCoCrAlY bond coat (BC) under thermomechanical loads were investigated by Rangaraj and Kokini, and it has been reported that thermal shock resistance is low in brittle materials like ceramic [3]. It has been found that failure mainly governed by the thermos-mechanic failures, chemical failures, erosion failures, oxidation of bond coat, hot erosion effect, CMAS ( $\text{CaO-MgO-Al}_2\text{O}_3\text{-SiO}_2$ ) attack, inconsistency in the thermal expansion, and due to changes in the thermal conductivity, etc. [4-9]. Thermal shock resistance changes with many properties such as fracture toughness, elastic modulus, Poisson's ratio, thermal expansion coefficient, and thermal conductivity. It has been investigated that thermal stresses that occur due to the temperature difference at the interface of the bond coat and surface of the specimen when cooled with water [10]. Few basic properties such as toughness, low thermal conductivity, stability at high temperature, high thermal expansion coefficient and low elastic modulus values are required to resist the thermal shock failure [11, 12]. Ceramic materials have the high-temperature resistant capacity so that it can be used in TBC systems to reduce the thermal shock failures. It satisfies basic properties such as toughness, low thermal conductivity, the coefficient of thermal expansion and low elastic module. Studies found that elastic modulus value changes with the closing or growth of cracks and plays a crucial role in the determination of TBC life. If crack growth increase, the value of the elastic module will change and that will hamper the TBC life period under service condition [13-15]. The failure of the coatings depends on the cracks, show when it propagates and results in failure. [16-18].

In the present investigation, an effort has been made to investigate the causes and mechanism behind the spallation of composite coating  $\text{Al}_2\text{O}_3\text{-ZrO}_2\cdot 5\text{CaO}$  applied to cast iron (CI) substrate of the particular thickness. The muffle furnace was used to heat and cool the coated sample uniformly during the thermal cyclic test. It is believed that the above studies are valuable for material scientists for the design of thermal-shock-resistant materials.

## II. EXPERIMENTAL METHODOLOGY

### 2.1. Selection of material and powder trade names

Cast iron (CI) was selected as a substrate material. The selection of powder was based on the thermal coefficient of expansion provided by Sulzer Metco. The trade names of different powders are shown in Table 1.

Table 1: Trade name and composition of the powder

Trade Name	Composition by wt. %
Metco 105 SFP	99.9% $\text{Al}_2\text{O}_3$
Metco 201 NS	$\text{ZrO}_2\cdot 5\text{CaO}$
Metco 452	$\text{Fe38Ni10Al}$

### 2.2. Coating Methodology

The Atmospheric plasma spray technique was used to coat on the cast iron substrate. Before the coating process, the mixture of  $\text{Al}_2\text{O}_3$  and  $\text{ZrO}_2\cdot 5\text{CaO}$  in 50:50 was prepared using ball mill technique. The substrates were chemically cleaned using tetra chloride-ethylene followed by preheating it to the temperature of  $250\pm 50$  °C. This process was done to minimize the thermal mismatch between the substrate and the bond coat. The schematic of a coating system is shown in Fig.1. The top coat thicknesses were about  $100\mu\text{m}$ . The plasma spray machine specification and spray parameters for bond coat and top coat are given in Table 2 and 3 respectively.

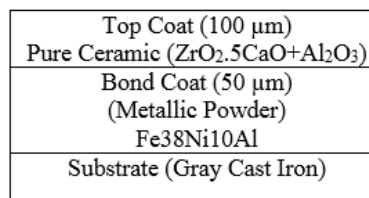


Fig.1 The schematic of coating system applied on CI substrate

Table 2: Air Plasma machine Specification

Specifications	Parameters
Plasma gun	3 Nylon Brush
Nozzle temperature	$10,000$ °C
Current	500 amps
Voltage	65-70 volts
Powder feed	45-50 gms/mint
Spray distance	50 -78 mm

Table 3 Plasma spray parameters for different coating materials.

Materials	Primary gas (Argon) Pressure(Bar)	Secondary gas (Hydrogen) Pressure (Bar)	Carrier gas Argon flow (lpm)	Current (amps)	Voltage (volts)	Spray distance (mm)
Al <sub>2</sub> O <sub>3</sub> + ZrO <sub>2</sub> .5CaO	3.7	3.45	35	500	65	65-76
Fe38Ni10Al	6.9	3.30	35	500	65	50-76

### 2.3. Thermal cyclic test procedure

The thermal cyclic test was conducted on a Muffle furnace. The schematic of the test setup shown in Fig.2. The temperature of the furnace was maintained at a temperature of  $600 \pm 2^\circ\text{C}$ . The coated substrate was kept on silica ceramic cups to ensure uniform heating all-around refer Fig.2. The heating and cooling cycle time of 30 minutes was maintained throughout the experiment. The cooling was done under ambient conditions.

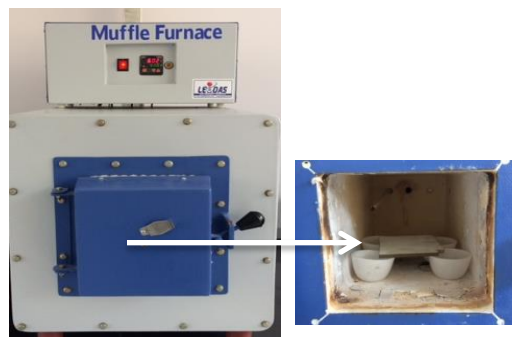


Fig. 2 Muffle furnace test setup

### 2.4 Coating characterization

Evaluation of the coating thickness, surface morphology, and determination of elemental composition was carried out using Zeiss Evo 18 special edition machine, and the machine specifications are given in Table 4. XRD analysis was carried out on Bruker, and its specifications are given in Table 5.

Table 4: Machine specifications of Zeiss Evo 18

Filament	Tungsten
Secondary e-image resolution	50 NM
Tilt	0 - 60 Degree
Rotation	360 Degree
EHT	200V - 30KV
Magnification	Up to 50K ~ 100K (Depends on sample)

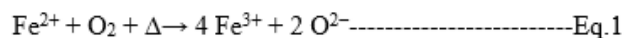
Table 5: X-ray Diffractometer specifications

Parameters	
Make	Bruker
Model	D8 Advance
Measuring circle diameter	435,500,600
Smallest addressable increment	0.0001°
Reproducibility	0.0001°
Anode	Cu
Detector	Scintillation & Lynxeye

### III. RESULTS AND DISCUSSIONS

Morphology of the as-sprayed and after thermal cyclic test shown in Fig. 3(a) and (b) respectively. The composite mixture applied as the top coat was found to be homogeneous, localized agglomeration, uneven microvoids, and localized pin holes. At higher magnification of 1500X, noticeable hair cracks were observed in the case of post-thermal cyclic test sample [Fig.3 b]. The cracks are formed in the alloyed mixture, mainly at the interfaces of the adjoining splats of the two different phases, alumina, and calcia stabilized zirconia, and hair crack impressions acknowledged mostly on the grains of Zirconia phase. The coefficient of thermal expansion value for alumina and zirconia dioxide are,  $9.6 \times 10^{-6} \text{ K}^{-1}$  &  $15.3 \times 10^{-6} \text{ K}^{-1}$  respectively [19]. The nucleation of these crack often attributed to the inconsistency in thermal coefficient of expansion between the two phases [20]. Also, due to the repeated thermal cyclic loading, i.e., heating and cooling residual compressive stresses institute in the composite mixture [21]. It is also evident from the micrograph that the network of cracks is more or less same in both the phases, Zirconia phase/grains (white color) and Alumina phase (dark gray color) identified as shown in Fig.3 b. The bulk stresses present in the bond coat decide the life of the coating, and the residual stresses present at the interface may interact with the micro defects and promote crack growth [22].

It is also evident that the top coat delaminated from the bond coat. The bond coat didn't spall from the substrate, and excellent metallurgical bonding understood. The reason of spallation of the top coat,  $\text{Al}_2\text{O}_3\text{-ZrO}_2\text{-5CaO}$  from the bond coat,  $\text{Fe38Ni10Al}$  attributed to the thermal inconsistency at the interface and effect amplified during prolonged heating and cooling cycle. It is also understood that the weakest link formed at the top/bond coat interface. Other reason for failure at the interface attributed to the differential porosity difference between the interfaces and roughness. The roughness at the interfaces act as stress concentrators and to a certain extent decides the lifespan of the coatings [23]. The average porosity for as-sprayed coating in case of the top coat and bottom coat found to be 1.90 & 2.75%, [Fig 4.c & d] respectively. The life of the coatings also found to depend on the porosity, horizontal and vertical cracks at the interface of the top/bond coat. LU et al. [24] had found that the presence of porosity is generally beneficial if a pre-existing crack dominates the failure. However, in the present work due to the porosity difference at the interface and the moisture present in the atmosphere leads to oxidation and can be visualized as dark black spots at the top coat [Fig.5 e]. EDX analysis has also confirmed the oxidation phenomenon. The elemental abundance of the individual elements, traces of iron content 1.51 wt. % along with oxygenated element 50.85 wt. % has been confirmed after thermal cyclic test refers to Fig. 6 h. No traces of any iron element found in case of as-sprayed coatings refer Fig.6 g. The oxidation at the top acknowledges due to the thermochemical reaction between the iron (Fe) elements present in the bond coat with the moisture present when exposed to ambient temperature during the thermal cyclic test [25]. The byproduct, rust formed at the surface can also be understood with the help of thermochemical, redox reaction given in Equation 1.



During the test, it was noticed that the thermally grown oxide layer (TGO) developed at the junction of the bond coat and top coat resulting weakening of the top coat/bond coat interface [Fig.8] The growth of the TGO layer found an increase with an increase in time. At the end of 312 cycles, the top coat starts delaminated from the edges shown in Fig.6 b. The failure of the coating in the present work is in agreement with results obtained by Julian D. Osorio [26].

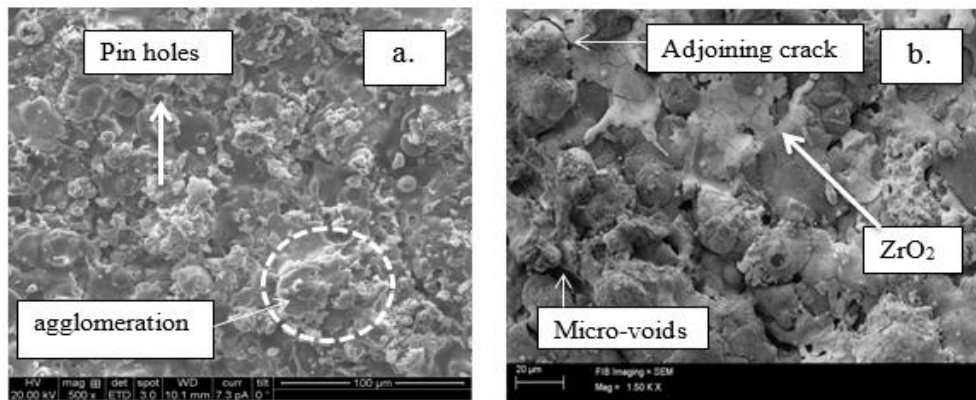


Fig.3 Morphology of the top coat (a) As-sprayed coating (b) After thermal cyclic test

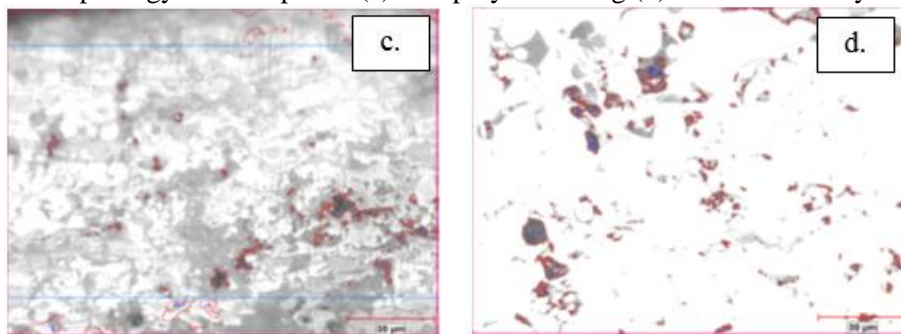


Fig.4 Micrograph of as-sprayed average porosity (c) 1.90 % topcoat and (d) 2.75% bond coat

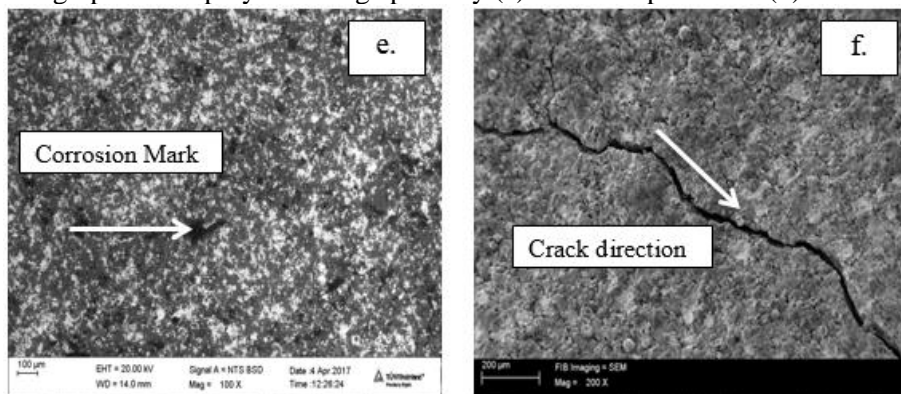


Fig.5 Micrograph of the topcoat post thermal cyclic test e. oxidation status after 295 cycle f. crack propagation after 312 thermal cycles test.

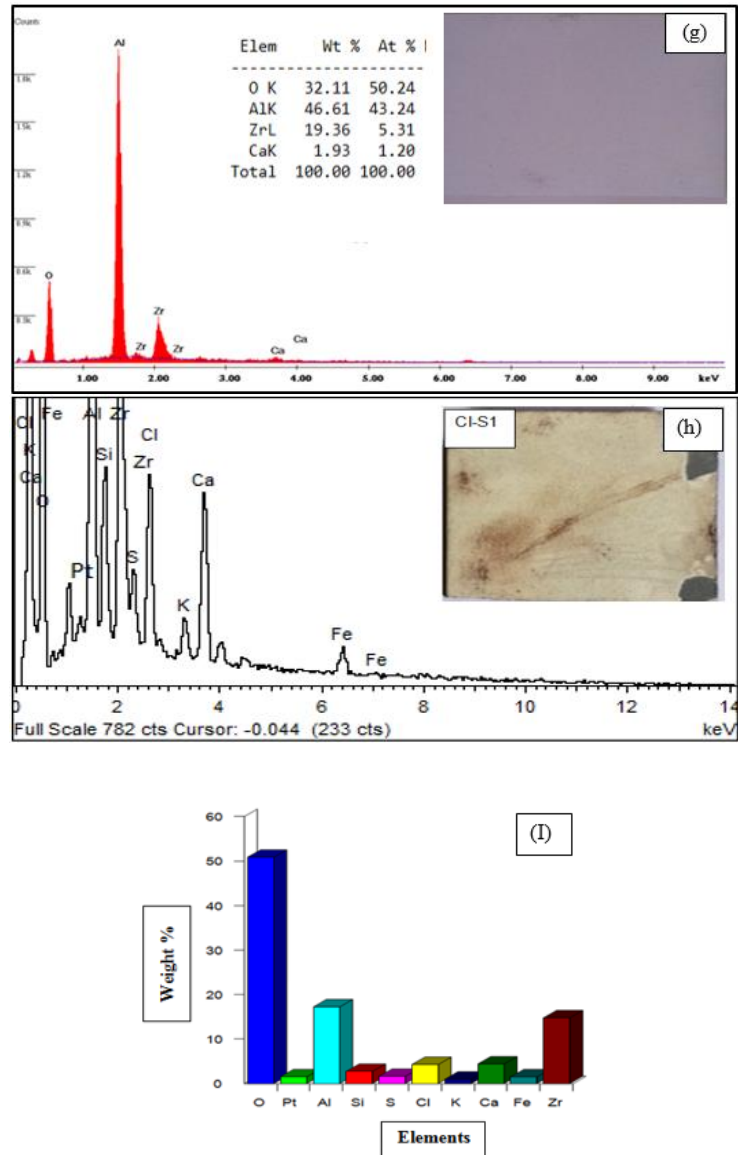


Fig.6 EDX and elemental composition of the topcoat (g): As-sprayed coatings (h)& (i): after thermal cyclic test.

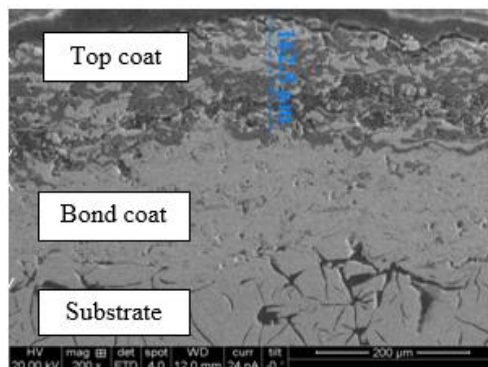


Fig.7 SEM micrograph (200X) at the cross section with no TGO layer between top coat/bond coat.

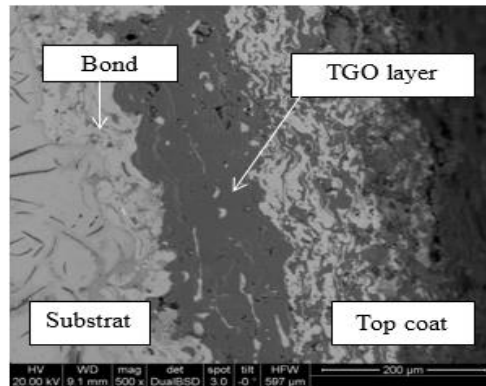


Fig. 8 SEM micrograph (500X) at the cross section with TGO layer between top coat/bond coat.

#### IV. CONCLUSION

The thermochemical effect found to play a crucial role and is having a detrimental impact on the life of the coating systems. No failure of the coating observed during constant heating as long as the specimen remained in the Muffle furnace. Bond coat shows excellent metallurgical bonding with the substrate. During prolonged heating and cooling cycle it is speculated that TGO, a brittle byproduct formed at the bond (Fe38Ni10Al) /top coat ( $\text{Al}_2\text{O}_3\text{-ZrO}_2\text{.5CaO}$ ) interfaces. Thermochemical and differential porosity at the interface found to develop the weakest link in the coating system also found governing mechanism behind spallation of the top coat. After 312 cycles the visible crack observed and considered as the failure of the top coat.

#### REFERENCES

- [1] Julian D. Osorio et al., “*Thermal barrier coatings for gas turbine applications failure mechanisms and key microstructural features*,” Medellin, December, :ResearchGate, 2012, pp. 149-158.
- [2] Saket Jaiswal, “*Synthesis of 3 Mol% Ytria Stabilized Zirconia (3YSZ) and Study on Corrosion Behavior of CMAS on Sintered 3YSZ Pellets*,” Bachelor of Technology in Ceramic Engineering, Department of Ceramic Engineering National Institute of Technology, Rourkela, 2015.
- [3] Sudarshan Rangaraj et al., “*Fracture in single layer (YSZ) – Bond Coat Alloy (NiCoCr10Al) composite coating under thermal shock*,” ScienceDirect, : Vol 52, Issue 2, 2004 pp. 455-465.
- [4] Liu J., “*Effects of bond coat surface preparation on thermal cycling lifetime and failure characteristic of thermal barrier coatings*,” Master of Science Thesis, Department of Mechanical, Materials, and Aerospace Engineering, University of Central Florida, Summer Term, 2004.
- [5] Verbeeck A.T.J., “*Plasma sprayed thermal barrier coatings: Production, characterization and testing*,” PhD Thesis, Technisch Universiteit Eindhoven, 1992.
- [6] Aygun A., “*Novel Thermal Barrier Coatings (TBCs) that are resistant to high Temperature attack by glassy deposits*,” The Ohio State University, ResearchGate, 2008.
- [7] Evans A.G., et al., “*Scaling laws governing the erosion and impact resistance of thermal barrier coatings*,” Wear, 2006, pp.886–894.
- [8] Wellman R.G., et al., “*Erosion, corrosion and erosion–corrosion of EB PVD thermal barrier coatings*,” Tribology International, 2008, vol.41 (7), 657-662.

- [10] Mao W.G., et al., “*Modeling of residual stresses variation With thermal cycling in thermal barrier coatings,*” ResearchGate, 2006, vol.38, pp.1118-1127.
- [11] Kara,I, E., “*TBK Kaplamaların Termal Şok Özelliklerinin İncelenmesi,*” Master Thesis,Sakarya University,” Metallurgical and Materials Engineering Department,Turkish, 2008.
- [12] Han J.C., et al., “*Thermal shock resistance of ceramics with temperature-Dependent material properties at elevated temperature,*” Acta Materiala, 2011, vol.59, pp.1373-1382.
- [13] Girolama G.D., et al., “*Microstructure, mechanical properties and thermal shock resistance of plasma sprayed nanostructured zirconia coatings,*” Ceramics International, 2011, 37, pp.2711-2717.
- [14] Siebert B., et al., “*Changes in porosity and Young's Modulus due to sintering of plasma sprayed thermal barrier coatings,*” Journal of Materials Processing Technology, 1999, 92-93, pp.217-223.
- [15] Yoshiba M., et al., “*High-Temperature Oxidation and Hot Corrosion Behavior of Two Kinds of Thermal Barrier Coating Systems for Advanced Gas Turbines,*” Journal of Thermal Spray Technology, 1996, vol. 5 (No. 3), 259-268.
- [16] Balint D.S., et al., “*An analytical model of rumpling in thermal barrier Coatings,*” Journal of the Mechanics and Physics of solids, 2005, vol. 53, pp.949–973.
- [17] Vaben R, Kerkhoff., et al., “*Development of a micromechanical life prediction model for plasma sprayed thermal barrier coatings,*” Materials Science and Engineering A, 2001, vol.303, pp. 100–109.
- [18] Yanar N.M., et al., “*Comparison of the Failures During Cyclic Oxidation of Yttria-Stabilized (7 to 8 Weight Percent) Zirconia Thermal Barrier Coatings Fabricated via Electron Beam Physical Vapor Deposition and Air Plasma Spray,*” Metallurgical and Materials Transactions A, 2011, vol. 42, pp . 905-921.
- [19] Guo H., et al., “*Effects of Heat Treatment on Microstructures and Physical Properties of Segmented Thermal Barrier Coatings,*” Materials Transactions, 2005,vol. 46, pp.1775-1778.
- [20] X.Q. Cao et al. “*Ceramic materials for thermal barrier coatings,*” Journal of the European Ceramic Society, vol. 24, Year 2004, pp. 1–10
  
- [21] Koshi Takenaka., “*Negative thermal expansion materials technological key for control of thermal expansion,*” Science and Technologyof Advance Materials.,2012, pp .11
- [22] D.M.Nisseley., “*Thermal Barrier Coatings Life Modeling in Aircraft Gas Turbine Engines,*” Jurnal of Thermal Spray Technlogy, vol.6, March 1997, pp.91-98.
- [23] Xiancheng Zhang et al., “*Effect of spraying condition and material properties on the residual stress in plasma spraying,*” Science and Technologyof Advance Materials., vol.20, 2004.
- [24] A.G Evans et al., “*Mechanical Behavior of Brittle Coatings on a Layer,*” Oxidation Metals.,vol.20, 1983, pp. 193-216.
- [25] T. J. L., et al., “*The thermal shock resistance of solids,*” Acta mater. vol. 46, No. 13, 1998 , pp. 4755-4768,
- [26] W.J.Brindley., et al., “*Surf.Coating Technol,*” vol.43/44,1990,pp.446-57.
- [27] Julian D. Osorio., et al., “*Thermal barrier coatings for gas turbine applications failure mechanisms and key microstructural features,*” Dyna, year 79, Nro.176, pp. 149-158. Medellin, December, 2012. ISSN 0012-7353.